

Interaction Notes

Note 623

30 June 2011

## **Electromagnetic Field Coupling to Transmission Lines Inside Rectangular Resonators**

S. Tkachenko\*, J. Nitsch\*, and R. Rambousky\*\*

\*Otto-von-Guericke-University-Magdeburg

\*\*Bundeswehr Research Institute for Protective Technologies and NBC Protection

### Abstract

In this paper the current inside a cavity, which is induced by lumped and distributed sources, is calculated. The current is obtained analytically (Green's function method) and numerically (MoM – and MLFMM – method). A long, parallel wire is chosen that connects two opposite walls of a rectangular resonator. Since the conductor conserves the translational symmetry of the resonator in one direction (z-direction), the current and the total exciting electrical field can be derived from Fourier series formulations. The obtained results clearly show the influence of the resonator on the induced current. Resonance peaks of the resonator, which do not arise in usual EMC laboratory tests, occur in the current spectra. The numerical results agree very well with the analytical ones, however, the results are obtained much faster using the analytical formulae - by a factor of one thousand.

<b>Contents</b>	<b>Page</b>
1. Introduction	3
2. Electromagnetic field coupling to a short-circuited thin wire maintaining the symmetry of the rectangular resonator	4
2.1 Resonator Green's functions	5
2.2 Calculation of the current	7
2.3 Determination of the function $S(\vec{\rho}, \vec{\rho}')$	8
3. Lumped and distributed sources (loads)	10
4. Transmission line approximation	13
5. Comparison of analytical and numerical results	15
6. Conclusion	18
References	19
Appendix I	21
Appendix II	25
Appendix III	26

## 1. Introduction

The performance of immunity tests according to current EMC standards on devices under laboratory conditions guarantees a certain basic protection for them. However, ultimately, these devices are used/installed in environments which do not correspond to the test environment in the laboratory. For example, they may be housed in shielded rooms and/or be connected in larger overall systems with other electrical and electronic components. In such cases, compliance of EMC standards for single devices/components does not mean EMC robustness of the total system, because in this system electromagnetic coupling may occur that was not present in the individual tests. In this paper this fact will be demonstrated analytically and numerically in a manageable, but not simple example.

Coupling of electromagnetic fields to different transmission-lines and antenna-like wiring structures is one of the main paths of interaction of intentional and natural electromagnetic interferences with electronic and electrical equipment. Usually such problems are considered for objects in free space [1], however, often such structures are inside resonator-like structures of a different kind (racks, cases, housings, fuselage of aircraft, etc.). Then, due to the presence of the resonator, the interaction can change greatly. Existing numerical methods (Method of Moments (MoM), Transmission-Line Matrix Method (TLM), etc.) allow considering specific cases only, but do not describe the general physical picture of the interaction. Thus, the analytical description of the interaction of high-frequency fields with wire structures in cavities has become a topic of interest (see, for example, [2]).

To solve this problem several methods can be offered. The approximate methods are based, as is usual in theoretical physics, on the use of small parameters. One group of such methods uses the smallness of the dimension of the wiring structure in comparison to the wavelength. This leads to the description of common modes of the scattered current with the aid of the model of small electrical dipole antennas [3, 4, 5] and to the differential modes of the scattered current using the method of small magnetic loop antennas [6]. The mutual influence of antenna and cavity modes increases with the length of the antenna. This influence can be quantitatively characterized by a shift of the resonance frequency of the system “antenna in cavity” in comparison with the resonance frequency of the empty cavity. It is proportional to the cube of the ratio of linear dimensions of the antenna and the cavity. Therefore, it follows that the maximal electromagnetic coupling occurs when the size of the antenna or transmission line is about the same size as the cavity.

Of course, for such a large extension of the scatterers, the “Method of Small Antenna” is not applicable. Another small parameter that can be used to solve the coupling problem for electrically long antennas and transmission lines inside a resonator is the thickness of the wire compared to other geometric parameters of the problem (wavelength, height of the wire above ground, etc.) [7]. The relevant mathematical technique is the method of analytical regularization [8] where the approximate resolution operator for the singular part of the Green’s function is given by the transmission line approximation, and the regular part of the Green’s function is defined by one or more eigenmodes of the cavity. This approach allows considering the coupling of electromagnetic fields with electrically long transmission lines and antennas of arbitrary geometric configuration inside the resonator, when the frequency is close to one of the resonance frequencies and all the other modes of the resonator contribute to form the singular part of the cavity’s Green’s function. This method was verified by comparison with results of the TLM method and yielded an acceptable agreement [7].

Further, in the publications [9,10,11] the method of analytical regularization is applied in implicit form. The authors of Ref. [9] only take the singular part of the cavity's Green's function in transmission-line approximation into account. This is also done in Ref. [10], but a finite sum of modes in the waveguide representation is chosen for the regular part of the Green's function.

It is interesting to check the method of Ref. [7] by comparing the results with the exact solution and to investigate the structure of the exact solution, even for special cases. Moreover, the problem can be used to investigate the change of the quality factor of the resonator caused by the presence of loaded transmission lines [12].

In this paper, for the exact solution of this problem a technique of theoretical physics is used for the investigation of a "wire in resonator" system that has *high symmetry*. This system consists of a rectangular resonator and an internal wire parallel to a resonator axis connecting opposite walls of the resonator. The wire can be loaded in an appropriate way (including two lumped loads near the terminals). Moreover, the method allows considering a finite number of such parallel (or perpendicular) wires. The electric field integral equation or mixed potential integral equation (using only the thin-wire approximation), which describes the induced current in such wires, can be solved by a Fourier transformation. The advantage of this geometry of the system leads to the similarity of the Fourier series expansion functions for the induced current and of the Fourier series expansion functions for the resonator Green's function in the direction of the wire. Moreover, during the investigation of the exact equation for the induced current one can separate terms corresponding to the transmission line approximation from those corresponding to cavity modes and evaluate the effect of different resonances.

The results of the analytical investigations were compared to numerical ones (MoM and Multi-Level Fast Multi-Pole Method (MLFMM) calculations) and a good agreement was found.

In conclusion, possible directions of future research are described. As is typical in theoretical physics, after using symmetry properties for some specific system one can generalize the results using a topological approach [13]. Note that from a topological point of view, the investigated transmission line with symmetric geometry is equivalent to a usual transmission line inside the resonator.

## **2. Electromagnetic field coupling to a short-circuited thin wire maintaining the symmetry of the rectangular resonator**

Consider a rectangular resonator with dimensions  $a, b, h$  (see Fig.1). In the resonator there is a wire that is parallel to four resonator walls and is perpendicular to the other two walls. The length of the wire  $L$  is equal to the distance  $h$  between the latter walls. Thus, the wire has the same geometric symmetry as the rectangular cavity. The wire can be loaded or (and) may have lumped sources localized near the walls. It is assumed that the radius of the wire,  $r_0$ , is small in comparison with all other dimensions of the problem (characteristic wavelength  $\lambda$ , dimensions of the resonator and distance between the wire and parallel walls).

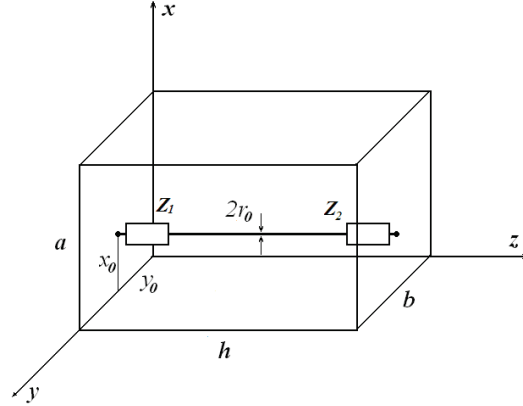


Fig. 1: Loaded symmetrical wire in the rectangular resonator with the parameters:  $a=1.5$  m,  $b=1.2$  m,  $h=0.9$  m. Length of the line  $L=h=0.9$  m, position of the line  $x_0=0.09$  m,  $y_0=0.37$  m, and  $r_0=1$  mm

It is also assumed that in the empty resonator (when the wire is absent) an electromagnetic field  $\vec{E}^0(\vec{r})$  is created in some way, e.g., by radiation of an additional antenna, the penetration of an external field through the slots and apertures of the cavity, etc. If the sources (current in the radiating antenna, dipole moments of the aperture, which can be treated as a current distribution) are known, the field in the resonator can be calculated by the Green's function formulation.

A central point in this paper is the calculation of the induced current  $I(z)$  along the conductor in the resonator. In order to achieve this, some intermediate steps are necessary.

### 2.1 Resonator Green's functions

Due to the assumed symmetrical wire configuration in the resonator, only the  $zz$  components of the dyadic Green's functions are relevant for the calculations here. This applies to the Green's function of the vector potential  $\vec{A}$  and for the scattered electric field  $E_{zz}^{sc}(\vec{r}, \vec{r}')$  in the ray – representation [14, 15]

$$G_{zz}^A(\vec{r}, \vec{R}) = \frac{\mu_0}{4\pi} \sum_{n_1, n_2, n_3 = -\infty}^{\infty} (-1)^{n_1+n_2} \frac{\exp(-jk|\vec{r} - \vec{R}(n_1, n_2, n_3)|)}{|\vec{r} - \vec{R}(n_1, n_2, n_3)|} \quad (1)$$

with

$$\begin{aligned} \vec{R}(n_1, n_2, n_3) &= (X(n_1), Y(n_2), Z(n_3)) \\ X(n_1) &= (-1)^{n_1} x_1 + \left( \frac{1 - (-1)^{n_1}}{2} + n_1 \right) a \\ Y(n_2) &= (-1)^{n_2} y_1 + \left( \frac{1 - (-1)^{n_2}}{2} + n_2 \right) b \\ Z(n_3) &= (-1)^{n_3} z_1 + \left( \frac{1 - (-1)^{n_3}}{2} + n_3 \right) h \end{aligned} \quad (2)$$

The coordinates  $x_1, y_1, z_1$  denote a point inside the resonator which is reflected  $n_1, n_2, n_3$  times at the resonator's walls in  $x, y,$  and  $z$  directions, respectively.

It can be shown that after some calculations – similar to those which have been performed in Ref. [16] -  $G_{zz}^A$  can be expressed as:

$$G_{zz}^A(\vec{r}, \vec{r}_1) = \frac{4\mu_0}{V} \sum_{\substack{n_1, n_2=1 \\ n_3=0}}^{\infty} \frac{\varepsilon_{n_3,0} \sin(k_{vx}x) \sin(k_{vx}x_1) \sin(k_{vy}y) \sin(k_{vy}y_1) \cos(k_{vz}z) \cos(k_{vz}z_1)}{k_v^2 - k^2 + j\delta} \quad (3)$$

with the abbreviations  $V = abh$ ,

$$\vec{k}_v = (k_{vx}, k_{vy}, k_{vz}), \quad k_{vx} = \frac{\pi}{a} n_1, \quad k_{vy} = \frac{\pi}{b} n_2, \quad k_{vz} = \frac{\pi}{h} n_3 \quad (4)$$

$$v := |n_1, n_2, n_3\rangle, \quad \delta \rightarrow +0, \quad \varepsilon_{n,m} = \begin{cases} 1, & m = n \\ 2, & m \neq n \end{cases}$$

The index  $v$  denotes an eigenstate (mode), e.g.  $TE_{011}$ , of the resonator. The bracket is adopted from quantum mechanics. The quantity  $\delta$  in the denominator is introduced in order to avoid singularities at the eigenfrequencies. It is mathematically necessary if eq. (7) would be transformed into time domain. Then, for the integration, the appropriate contour goes around the singularity, and  $\delta$  is the distance of the contour to the pole. In a physical sense  $\delta$  can be assigned to small losses in the resonator, like, e.g. losses in the walls. In any case it has the same dimension as  $k^2$ .

It can further be shown that the above summation over three indices can be reduced and simplified to a sum over two.

The vector potential Green's function  $\hat{G}^A$  of the resonator is connected with the dyadic Green's function of the electric field [17] via the equation

$$\hat{G}^E(\vec{r}, \vec{r}') = \frac{1}{j\omega\varepsilon_0} (k^2 + \text{grad}_{\vec{r}} \text{div}_{\vec{r}}) \hat{G}^A(\vec{r}, \vec{r}') \quad (5)$$

Therefore, for the  $zz$  – component  $G_{zz}^E$  it follows

$$G_{zz}^E(\vec{r}, \vec{r}') = \frac{\eta_0 c}{jk} \left( k^2 + \frac{\partial^2}{\partial z^2} \right) G_{zz}^A(\vec{r}, \vec{r}') \quad (6)$$

Here  $c$  denotes the speed of light and  $\eta_0 = \sqrt{\mu_0/\varepsilon_0}$ .

Inserting eq. (3) into eq. (6) and performing the differentiation leads to

$$G_{zz}^E(\vec{r}, \vec{r}_1) = \frac{4\eta_0}{jkV} \sum_{\substack{n_1, n_2=1 \\ n_3=0}}^{\infty} \frac{\varepsilon_{n_3,0} (k^2 - k_{vz}^2) \sin(k_{vx}x) \sin(k_{vx}x_1) \sin(k_{vy}y) \sin(k_{vy}y_1) \cos(k_{vz}z) \cos(k_{vz}z_1)}{k_v^2 - k^2 + j\delta} \quad (7)$$

By virtue of the chosen symmetry of the conductor relative to the resonator walls the  $zz$  – component of the Green's function  $\hat{G}^E$  is sufficient to calculate the (scattered) current along

the line. If the exciting field  $\vec{E}^0(\vec{r})$  inside the resonator is known, then the induced (scattered) current  $I(z)$  is related to scattered electric field by

$$E_z^{sc}(\vec{r}) = \int_0^h G_{zz}^E(\vec{r}, \vec{r}') I(z') dz' \quad (8)$$

And, in addition to the boundary conditions on the surface of the conductor for the total electric field, the current can be calculated.

## 2.2 Calculation of the current

It is assumed that both ends of the conductor are directly connected with the corresponding walls, i.e. the conductor is short circuited at both ends. Furthermore, only the component of the exciting field parallel to the conductor  $E_z^0$  couples to the line, and it also has to fulfill the boundary conditions on the resonator walls. For this reason, it factorizes with respect to its coordinates as follows:

$$E_z^0(\vec{r}) = \sum_{n_3=0}^{\infty} E_{zn_3}^0(x, y) \cdot \cos(n_3\pi z / h) \quad (9)$$

If one additionally uses the fact that the conductor is short – circuited, the current can be written as

$$I(z) = \sum_{n_3=0}^{\infty} I_{n_3} \cos(n_3\pi z / h) \quad (10)$$

and one immediately obtains  $dI/dz|_{z=0} = dI/dz|_{z=h} = 0$ . On the basis of equations (9) and (10) together with the boundary condition for the total electrical field on the surface of the conductor<sup>1</sup>

$$E_z^{sc}(x_0 + r_0, y_0, z) + E_z^0(x_0 + r_0, y_0, z) = 0, \text{ (here } r_0 \text{ is the radius of the wire)} \quad (11)$$

one can derive the unknown expansion components  $I_{n_3}$  for the current. This is carried out in the next step. Remember  $E_z^{sc}(x_0 + r_0, y_0, z)$  is given by

$$E_z^{sc}(x_0 + r_0, y_0, z) = \int_0^h G_{zz}^E(x_0 + r_0, y_0, x_0, y_0, z') I(z') dz' \quad (12)$$

---

<sup>1</sup> For the derivation the thin – wire approximation is used. Then, the radius of the wire is much smaller than all other characteristic lengths of the problem: wavelength, length of the wire, distances from the wire to the walls of the resonator. In this approximation it is assumed: 1. The current has only an axial component (the azimuthal component is zero); 2. The current is concentrated in the filament coinciding with the wire axis (see eq. (12)); 3. The zero-boundary condition for the tangential component of the total electric field has to be satisfied for each  $z$  at least in the immediate vicinity of the boundary of the wire (see eq. (11)).

In reality the current also has an azimuthal component. The current density for both components is distributed along the boundary of the perfectly conducting wire, and the zero - boundary condition for the tangential as well as for the azimuthal component of the total field has to be satisfied at any point of the boundary of the wire.

Calculating this integral with the aid of (7) and (10) and using eq. (11), one can resolve the resulting (longer) equation with respect to the components  $I_{n_3}$

$$I_{n_3} = - \frac{E_{zn_3}^0(x_0 + r_0, y_0)}{jkab \sum_{n_1, n_2=1}^{\infty} \frac{(k^2 - k_{vz}^2) \sin(k_{vx}(x_0 + r_0)) \sin(k_{vx}x_0) \sin^2(k_{vy}y_0)}{k_v^2 - k^2 + j\delta}} \quad (13)$$

Inserting the expansion components  $I_{n_3}$  in the series of eq.(10) one obtains the current  $I(z)$  along the line.

Note that eqs. (13) and (10) yield an exact solution of the Electrical Field Integral Equation (EFIE) (11) for arbitrary exciting fields (they can be distributed, lumped, or may contain both components, distributed as well as lumped, see below).

Next, it is of interest to simplify the double sum in the denominator (13) in order to speed up necessary numerical calculations and to derive a connection with a corresponding transmission-line approximation. To do this, the function  $S$  must be defined as

$$S = S(k, \vec{\rho}, \vec{\rho}') := \frac{4}{ab} \sum_{n_1, n_2=1}^{\infty} \frac{\sin(k_{vx}x) \sin(k_{vx}x') \sin(k_{vy}y) \sin(k_{vy}y')}{k_{v\rho}^2 + k_{vz}^2 - k^2 + j\delta} \quad (14)$$

with  $\vec{\rho} = (x, y)$ ,  $\vec{k}_{v\rho} = (k_{vx}, k_{vy})$ .

Then eq. (13) reads

$$I_{n_3} = \frac{jkE_{zn_3}^0(x_0, y_0)}{\eta_0(k_{vz}^2 - k^2) S(x = x_0 + r_0, y = y_0, x' = x_0, y' = y_0)} \quad (15)$$

In the following step the function  $S(\vec{\rho}, \vec{\rho}')$  shall be estimated.

### 2.3 Determination of the function $S(\vec{\rho}, \vec{\rho}')$ .

The sine products in eq. (14) are rewritten in differences of cosine functions and subsequently completed to exponential functions. Then, this results in a product of two sinuses:

$$S(\vec{\rho}, \vec{\rho}') = \frac{1}{4ab} \sum_{n_1=-\infty}^{\infty} \frac{e^{-jk_{vx}(x-x')} - e^{jk_{vx}(x+x')}}}{k_v^2 - k^2 + j\delta} \sum_{n_2=-\infty}^{\infty} \left( e^{-jk_{vy}(y-y')} - e^{jk_{vy}(y+y')} \right) \quad (16)$$

This expression, in turn, can be artificially enlarged by two integration processes

$$S(\vec{\rho}, \vec{\rho}') = \int_{-\infty}^{\infty} d\tilde{k}_x \int_{-\infty}^{\infty} d\tilde{k}_y \sum_{n_1=-\infty}^{\infty} \delta(\tilde{k}_x - k_{vx}) \cdot \sum_{n_2=-\infty}^{\infty} \delta(\tilde{k}_y - k_{vy}) \cdot \frac{\left( e^{-j\tilde{k}_x(x-x')} - e^{j\tilde{k}_x(x+x')} \right) \left( e^{-j\tilde{k}_y(y-y')} - e^{j\tilde{k}_y(y+y')} \right)}{\tilde{k}_\rho^2 + k_{vz}^2 - k^2 + j\delta} \quad (17)$$



with the advantage that the sums over the  $\delta$  - functions can be replaced by a sum of exponential functions, like, e.g.,

$$\sum_{n_1=-\infty}^{\infty} \delta(\tilde{k}_x - k_{vx}) = \sum_{n_1=-\infty}^{\infty} \delta(\tilde{k}_x - 2\pi n_1 / 2a) = \frac{a}{\pi} \sum_{n_1=-\infty}^{\infty} e^{j2\tilde{k}_x n_1 a} \quad (18)$$

and, likewise, the other sum. One then has to collect all exponential functions in a proper way to end up with an integral, like

$$\frac{1}{(2\pi)^2} \int d\tilde{k}_\rho \frac{\exp(j\tilde{k}_\rho \cdot \vec{\rho})}{\tilde{k}_\rho^2 + k_{vz}^2 - k^2 + j\delta} \quad (19)$$

as the essential part behind the double sum.

Integration over the angle  $\varphi_k$  (in the  $k$  -space) yields [18]

$$\begin{aligned} \frac{1}{(2\pi)^2} \int \frac{\tilde{k}_\rho d\tilde{k}_\rho}{\tilde{k}_\rho^2 + k_{vz}^2 - k^2 + j\delta} \int_0^{2\pi} \exp(j\tilde{k}_\rho \rho \cos \varphi_k) d\varphi_k = \\ = \frac{1}{(2\pi)^2} \int \frac{\tilde{k}_\rho J_0(\tilde{k}_\rho \rho) d\tilde{k}_\rho}{\tilde{k}_\rho^2 + k_{vz}^2 - k^2 + j\delta} =: I_\rho \end{aligned} \quad (20)$$

Here  $J_0(\tilde{k}_\rho \rho)$  denotes the Bessel function of zeroth order. This integral has an exact solution and results in [19]

$$I_\rho = \frac{1}{2\pi} \begin{cases} K_0(\rho \underbrace{\sqrt{k_{vz}^2 - k^2}}_{=: \gamma_{vz}}), & k_{vz}^2 - k^2 > 0 \\ -\frac{j\pi}{2} H_0^{(2)}(\rho \underbrace{\sqrt{k^2 - k_{vz}^2}}_{=: \tilde{k}_{vz}}), & k^2 - k_{vz}^2 < 0 \end{cases} \quad (21)$$

The functions  $K_0$  and  $H_0^{(2)}$  in (21) are a cylindrical function of imaginary argument and a Hankel function of second kind, respectively. Now the final result for  $S$  can be written very compactly:

$$S = \frac{1}{2\pi} \sum_{n_1, n_2=-\infty}^{\infty} (-1)^{n_1+n_2} \begin{cases} K_0(\gamma_{vz} | \vec{\rho} - \vec{\rho}(n_1, n_2) |), & k_{vz}^2 - k^2 > 0 \\ -\frac{j\pi}{2} H_0^{(2)}(\tilde{k}_{vz} | \vec{\rho} - \vec{\rho}(n_1, n_2) |), & k^2 - k_{vz}^2 < 0 \end{cases} \quad (22)$$

with the definition

$$\vec{\rho}(n_1, n_2) = (X(n_1), Y(n_2)) \quad (23)$$

The quantities  $X(n_1)$  and  $Y(n_2)$  are taken from eq. (2). Insertion of the above function  $S$  into eq. (15) leads to the final result for the expansion coefficients of the current and thus, via eq. (10), to the current along the conductor<sup>2</sup>.

<sup>2</sup> The representation (22) of the function  $S$  has a clear physical meaning. This is a two-dimensional scalar Green's function for a filament source with frequency  $c\tilde{k}_{vz}$  inside a two dimensional rectangular cavity which is obtained by the reflection method. It also can be

The representation (22) of the function  $S$  has a clear physical meaning. This is a two-dimensional scalar Green's function of a filament source with frequency  $ck_{vz}$  inside a two dimensional rectangular cavity that is obtained by the reflection method (see Fig.2). It also

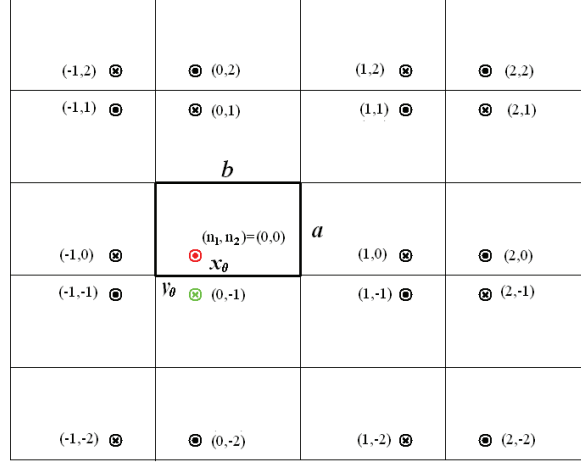


**Fig. 2** Mirror procedure for the filament source in a 2-dimensional rectangular resonator

can be considered as a part of a hybrid representation of the  $zz$  component of the Green's function for the vector potential (exponential or trigonometric function for the  $z$  - direction and cylindrical function for the  $\rho$  - direction). (For the free space such representation can be found, for example, in the book [17], Chapter 2.2). This representation is especially convenient when the source and the observation point (for two dimensional problems) are closely adjacent and one needs to extract the spatial-divergent part to obtain the transmission line approximation (see below). Of course, representation (22) is not unique. One can obtain another representation using the apparatus of theta-functions (see Appendix I). This representation is convenient for the investigation of resonances in frequency domain. Another representation of the function  $S$  can be obtained by carrying out the summation over one index in eq. (14) using the known formulas of Fourier series (see Appendix II). This representation is convenient for numerical calculations.

Note that so far the excitation of the short-circuited wire in the resonator took place by a distributed field. If lumped sources should additionally feed the conductor, then additional currents arise from these sources. This situation is the subject of the next section.

### 3. Lumped and distributed sources (loads)

In this section it is assumed that besides an exterior electric field lumped sources (at one or both ends of the conductor) may also excite the line. A lumped source at the left hand side of the line is represented as <sup>3</sup>

---

considered as a part of a hybrid representation of the  $zz$  component of the Green's function for the vector potential (exponential or trigonometric function for the  $z$  - direction and cylindrical function for the  $\rho$  - direction). (For the free space such representation can be found, for example, in the book [17], Chapter 2.2). This representation is especially convenient when the source and the observation point (for two dimensional problems) are close to one another, and one needs to extract the spatial-divergent part to obtain the transmission line approximation (see below). Of course, representation (22) is not unique. One can obtain another representation by carrying out one summation in [14] and using, for example, the method described in [1]; or another representation by using the apparatus of theta-functions (see Appendix).

<sup>3</sup> Below it is assumed that the distance between the source and wall of the resonator is about the dimension of the source.

$$E_{z,l}^0(x_0, y_0, z) = U_l \delta(z - \Delta), \quad \Delta \rightarrow 0 \quad (24)$$

with some voltage amplitude  $U_l$  ( $l = \text{left}$ ).

Then one can write

$$U_l \delta(z - \Delta) = \sum_{n_3=0}^{\infty} E_{z,l,n_3}^0 \cos(n_3 z \pi / h) \quad (25)$$

Multiplying both sides of eq. (25) with  $\cos(\tilde{n}_3 z \pi / h)$  and performing an integration over the coordinate  $z$  from  $0$  to  $h$ , one finally finds for the expansion coefficients of the field  $E_{z,l}^0$ :

$$E_{z,l,n_3}^0 = \varepsilon_{n_3,0} \frac{U_l}{h} \cos(n_3 \Delta \pi / h) \quad (26)$$

Insertion of eq. (26) into eq. (15) yields for the current  $I_l(z)$  that emerges from the left  $\delta$ -source (for  $\Delta \rightarrow 0$ )

$$I_l(z) = \frac{jkU_l}{\eta_0 h} \sum_{n_3=0}^{\infty} \frac{\varepsilon_{n_3,0} \cos(\pi n_3 z / h)}{(k_{vz}^2 - k^2) S} =: U_l Y_l(z) \quad (27a)$$

The summation is carried out up to some maximal index  $N_3$  which is of the order  $N_3 \sim h / \Delta$  (this restriction corresponds to the fact that wavelengths are assumed to be larger than the dimension of the source)

If the lumped source is positioned at the right hand side of the wire one similarly obtains for the current  $I_r(z)$  created on the wire:

$$I_r(z) = \frac{jkU_r}{\eta_0 h} \sum_{n_3=0}^{\infty} \frac{\varepsilon_{n_3,0} (-1)^{n_3} \cos(\pi n_3 z / h)}{(k_{vz}^2 - k^2) S} =: U_r Y_r(z) \quad (27b)$$

If the investigated line contains lumped impedances they also can be treated as lumped sources that cause a jump in the potential (which is considered to be static for small distances) in a region  $\sim \Delta$ . In other words, they can be considered as lumped sources with unknown amplitudes (that have to be determined by the solution of a system of linear equations, see below) [20]:

$$E_{z,l}^0(x_0, y_0, z) = -Z_1 I(\Delta) \delta(z - \Delta) \approx -Z_1 I(0) \delta(z - \Delta) \Rightarrow U_l = -Z_1 I(0) \quad (28a)$$

$$E_{z,r}^0(x_0, y_0, z) = -Z_2 I(h - \Delta) \delta(z - h + \Delta) \approx -Z_2 I(h) \delta(z - h + \Delta) \Rightarrow U_r = -Z_2 I(h) \quad (28b)$$

Due to the validity of the superposition principle of electrodynamics one can represent the total exciting field  $E_{z,t}^0$  of the wire and the total current  $I(z)$ , respectively:

$$E_{z,t}^0(z) = -Z_1 I(0) \delta(z - \Delta) - Z_2 I(h) \delta(z - h + \Delta) + E_z^0(z) \quad (29)$$

$$I(z) = I_l(z) + I_r(z) + I_f(z) \quad (30)$$

Here  $I_f(z)$  is the contribution of the current that is generated by the exterior electric field  $E_z^0(z)$

$$I_f(z) = \frac{jk}{\eta_0} \sum_{n_3=0}^{\infty} \frac{E_{z,n_3}^0(x_0, y_0)}{(k_{vz}^2 - k^2) \cdot S} \cos(\pi n_3 z / h) \quad (31)$$

The quantity  $Z_1$  denotes the input - and the quantity  $Z_2$  the output impedance.

Now the current can be calculated at every point  $(x_0, y_0, z)$  on the conductor. Of particular interest are the current values at the beginning ( $I(0)$ ) and at the end ( $I(h)$ ) of the line. By virtue of eq. (30), together with the corresponding expressions for the partial currents, one obtains:

$$I(0) = \frac{I_f(0)[1 + Z_2/Z_{00}] - I_f(h)Z_2/Z_{01}}{[1 + Z_1/Z_{00}][1 + Z_2/Z_{00}] - Z_1Z_2/(Z_{01})^2} \quad (32)$$

and

$$I(h) = \frac{I_f(h)[1 + Z_1/Z_{00}] - I_f(0)Z_1/Z_{01}}{[1 + Z_1/Z_{00}][1 + Z_2/Z_{00}] - Z_1Z_2/(Z_{01})^2} \quad (33)$$

The symmetry between these equations is obvious. Both denominators are equal. The nominators can be transformed into each other by exchanging the input and output impedances and the currents  $I_f(0) \leftrightarrow I_f(h)$ . The newly appearing quantities  $Z_{00}$  and  $Z_{01}$  denote impedances that are defined by

$$(Z_{00})^{-1} := Y_l(0) = Y_r(h) \quad (Z_{01})^{-1} := Y_l(h) = Y_r(0) \quad (34)$$

Note that all partial currents have the common quotient

$$\cos(\pi n_3 z / h) \cdot [(k_{vz}^2 - k^2)S]^{-1} \quad (35)$$

behind the sum sign. Therefore they have the same poles (zeros in the denominator), which describe resonance phenomena of the (total) current. One can observe that the resonances depend on the geometry of the resonator and conductor and on frequency ( $k$ ), the location on the line  $(x_0, y_0)$  and the loads of the line  $Z_1$  and  $Z_2$ . This is an important fact which has to be taken into account when testing devices under EMC aspects.

#### 4. Transmission line approximation

In this section it shall be shown that the lowest order approximation of the essential factor  $S$  is based on the well-known (classical) transmission line equations<sup>4</sup>. In order to derive this limit the subsequent assumptions for the validity of transmission line approximation are made:

$$|\gamma_{vz}| \cdot |\vec{\rho} - \vec{\rho}_0| = |\gamma_{vz}| r_0 \ll 1, \quad |\gamma_{vz}| x_0 \ll 1 \quad (36)$$

Furthermore, it is assumed that the wire is located far enough from the other walls of resonator:  $x_0 \ll a, b, y_0$ .

Then the leading two terms ( $n_1 = n_2 = 0$ ;  $n_1 = -1, n_2 = 0$ , see red “source” and green “main mirror” in Fig.2) of the sum for  $S$  in eq. (22) are pulled out of the sum sign:

$$S(k, k_{vz}, \vec{\rho}, \vec{\rho}') = \frac{1}{2\pi} \left\{ K_0(\gamma_v | \vec{\rho} - \vec{\rho}' |) - K_0(\gamma_v | \vec{\rho} - \vec{\rho}'(-1,0) |) \right. \\ \left. - j\pi/2 [H_0^{(2)}(\tilde{k}_{vz} | \vec{\rho} - \vec{\rho}' |) - H_0^{(2)}(\tilde{k}_{vz} | \vec{\rho} - \vec{\rho}'(-1,0) |)] \right\} + \quad (37) \\ + \frac{1}{2\pi} \sum_{\substack{n_1, n_2 = -\infty \\ n_2 \neq 0, n_1 \neq 0, 1}}^{\infty} (-1)^{n_1 + n_2} \begin{cases} K_0(\gamma_{vz} | \vec{\rho} - \vec{\rho}(n_1, n_2) |), & k_{vz}^2 - k^2 > 0 \\ -\frac{j\pi}{2} H_0^{(2)}(\tilde{k}_{vz} | \vec{\rho} - \vec{\rho}(n_1, n_2) |), & k_{vz}^2 - k^2 < 0 \end{cases}$$

and the function  $S(x = x_0 + r_0, y = y_0, x' = x_0, y' = y_0)$  in (15) is approximated by the natural logarithm function  $\rightarrow \ln(2x_0/r_0)$ . Thus one obtains the known logarithmic divergence of the TL theory:

$$S_{TL} = \frac{1}{2\pi} \ln(2x_0/r_0) \quad (38)$$

Using this function in all expressions for the fields, currents, admittances, etc. leads to corresponding equations for the TL theory in the resonator. This is shown in the following for all partial currents. First  $Y_l^{TL}(z)$  is considered (see eq. 27 a)

$$Y_l^{TL}(z) = \frac{jk}{\eta_0 h} \frac{2\pi}{\ln(2x_0/r_0)} \cdot \sum_{n_3=0}^{\infty} \frac{\varepsilon_{n_3,0} \cos(n_3 \pi z / h)}{(\pi n_3 / h)^3 - k^2} = \frac{jk}{h Z_C} \cdot \sum_{n_3=-\infty}^{\infty} \frac{\exp(n_3 \pi z / h)}{(\pi n_3 / h)^3 - k^2} \quad (39)$$

Here the characteristic impedance is introduced

$$Z_C = \frac{\eta_0}{2\pi} \ln(2x_0/r_0) \quad (40)$$

The function  $Y^{TL}(z)$  fulfills a differential equation of second order

---

<sup>4</sup> The limiting case  $a, b, h, y_0 \rightarrow \infty$  (but for finite value of  $x_0$ ) leads to the well-known result for the coupling of an electromagnetic field to an infinite horizontal wire above perfectly conducting ground (see Appendix III).

$$\left(d^2/dz^2 + k^2\right)Y^{TL}(z) = -\frac{jk}{hZ_C} \sum_{n_3=-\infty}^{\infty} \exp(jn_3\pi z/h) \quad (41)$$

The fact that the sum in eq. (41) can be represented as  $\delta$  - function yields

$$\left(d^2/dz^2 + k^2\right)Y^{TL}(z) = -\frac{jk}{Z_C} \delta(z) \quad (42)$$

with 
$$Y_l^{TL}\Big|_{0+} - Y_l^{TL}\Big|_{0-} = -\frac{2jk}{Z_C}$$

This was expected since the current  $I_l^{TL}(z) = U_l Y_l^{TL}(z)$  is generated by a  $\delta$  - source. Solving the above differential equation or summing up directly eq. (39) for  $Y_l^{TL}(z)$  results in [18]

$$Y_l^{TL}(z) = \frac{jk}{Z_C h} \left(\frac{h}{\pi}\right)^2 \left[ -\frac{1}{k^2} + 2 \sum_{n_3=1}^{\infty} \frac{\cos(n_3\pi z/h)}{n_3^2 - (kh/\pi)^2} \right] = -\frac{j}{Z_C} \frac{\cos(k(h-z))}{\sin(kh)} \quad (0 \leq z \leq h) \quad (43)$$

Note that the zeros in the denominator now only depend on the conductor length and frequency. In this limit the wire does not interact with the resonator.

Analogously, one derives for the current that is generated by the right hand side  $\delta$  - source the result:

$$Y_r^{TL}(z) = -\frac{j}{Z_C} \frac{\cos(kz)}{\sin(kh)} \quad (0 \leq z \leq h) \quad (44)$$

An interesting case of these intermediate results is the application on a line which is fed by a source at the left and terminated at the end by impedance  $Z_2$ . Then the (total) current reads

$$I(z) = U_l Y_l(z) - Z_2 I(h) Y_r(z) \quad (45)$$

From this it is easy to obtain the current at the beginning and at the end of the conductor

$$I(0) = U_l \left[ Y_l(0) - Z_2 \frac{Y_l(h)}{1 + Z_2 Y_r(h)} Y_r(0) \right] = U_l \frac{Y_l(0) + Z_2 [Y_l^2(0) - Y_l^2(h)]}{1 + Z_2 Y_l(0)} \quad (46a)$$

$$I(h) = \frac{U_l Y_l(h)}{1 + Z_2 Y_l(0)} \quad (46b)$$

for the exact result and

$$I^{TL}(0) = \frac{U_l}{jZ_C} \frac{Z_c j \cos(kh) - Z_2 \sin(kh)}{Z_c j \sin(kh) + Z_2 \cos(kh)}; \quad I^{TL}(h) = \frac{U_l}{Z_c j \sin(kh) + Z_2 \cos(kh)} \quad (47a,b)$$

for the result in TL - approximation.

It remains to calculate the field generated current  $I_f(z)$  in the TL – limit. One starts with

$$I_f^{TL}(z) = \frac{jk}{Z_C h} \sum_{n_3=0}^{\infty} \frac{E_{z,n_3}^0 \cos(\pi n_3 z / h)}{(n_3 \pi / h)^2 - k^2} \quad (48)$$

Inserting

$$E_{z,n_3}^0 = \frac{\varepsilon_{n_3,0}}{h} \int_0^h E_z^0(z') \cos(\pi n_3 z' / h) dz' \quad (49)$$

into eq. (48) one gets

$$I_f^{TL}(z) = \int_0^h E_z^0(z') dz' \underbrace{\frac{jk}{Z_C h} \sum_{n_3=0}^{\infty} \frac{\varepsilon_{n_3,0} \cos(\pi n_3 z / h) \cos(\pi n_3 z' / h)}{(n_3 \pi / h)^2 - k^2}}_{g^{TL}(z, z', h)} \quad (50)$$

Note that the term with the sum in the integral represents the Green's function  $g^{TL}(z, z', h)$  in TL approximation (for the short-circuited horizontal line). Based on known formulas (see, e.g., [18]) one can perform the summations and finally obtains

$$g^{TL}(z, z', h) = -\frac{j}{Z_C \sin(kh)} \begin{cases} \cos(k(h-z)) \cos(kz'), & z' \leq z \\ \cos(k(h-z')) \cos(kz), & z' \geq z \end{cases} \quad (51)$$

As expected, this Green's function and current fulfill the following differential equations

$$\left( \frac{d^2}{dz^2} + k^2 \right) \begin{cases} g^{TL}(z, z', h) \\ I_f^{TL}(z) \end{cases} = -\frac{jk}{Z_C} \begin{cases} \delta(z' - z) \\ E_z^0(z) \end{cases} \quad (52)$$

This concludes the investigations in the transmission line – limit. It should be emphasized that in the TL approximation there is no interference between chamber and conductor (except the boundary conditions). If, however, the frequency is in the neighborhood of an eigenfrequency of the resonator or the conditions (36) are violated, strong interaction between resonator and wire will occur. This situation is investigated in the next section.

## 5. Comparison of analytical and numerical results

This section serves for the comparison of analytical and numerical results which are obtained by both application of the above formalism to calculate the induced current on the line as well as by numerical calculations using the program packages CONCEPT II (MoM - method) [21] and PROTHEUS (MLFMM – procedure) [22]. A lumped source at the beginning of the line was chosen as the exciting (ideal) source with  $U_0=1$  V. At the far end the line was terminated with 1, 50, 311 (see eq.(40)), and  $10^5$  Ohm (short-circuit, 50 Ohm, “matched”  $Z_2 = Z_c$ , and open-circuit), respectively. For all these configurations the input impedance of the line was determined in the frequency range between 50 and 500 MHz. It is worth noting that each of these calculations took about 20 hours on a powerful parallel computer (IBM X3850 M2, calculation with 30 processors), whereas the computation time for the analytical calculation

was about 2 minutes. Note that the maxima of the input impedance correspond to the minima of the input current and vice versa.

In addition to the exact analytical and numerical results, results were also obtained in the transmission – line limit (see eqs. in Section 4). For the numerical calculation in this limit the conductor above ground plane was chosen to connect two walls in an otherwise free space. In order to not overload this work with too many figures, only results with  $Z_2 = 50 \Omega$  are displayed. In Fig. 2 and Fig. 3 all occurring resonances can be identified. For example, the resonances at 160 MHz, 231 MHz, 236 MHz, 269 MHz, and 289 MHz successively correlate with the modes  $v := |n_1, n_2, n_3\rangle = |1,1,0\rangle, |1,1,1\rangle, |2,1,0\rangle, |1,2,0\rangle,$  and  $|2,1,1\rangle$  of the cavity. At these frequencies the input current has maxima which arise due to the strong coupling between cavity walls and conductor.

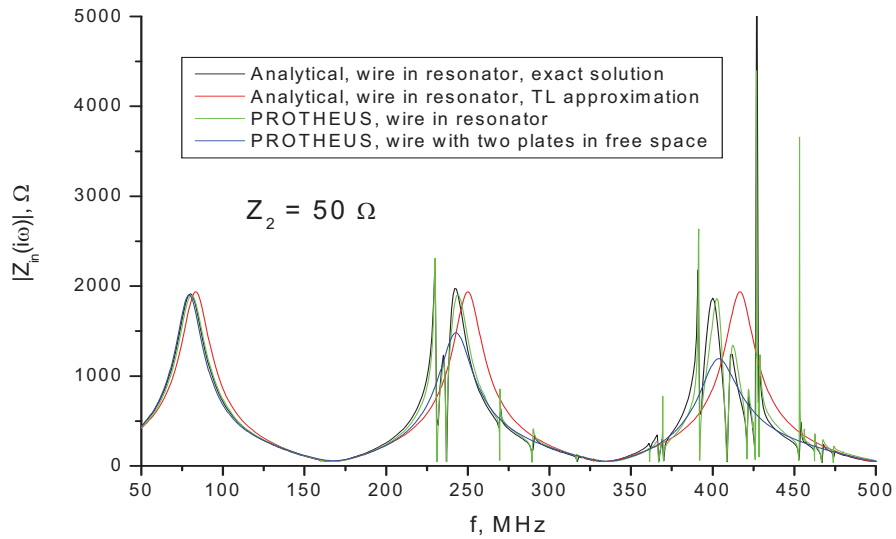


**Fig. 3** Frequency dependency of the input impedance

It can be recognized that the results obtained with the aid of the program package PROTHEUS agree quite well with the analytical results, whereas those calculated with CONCEPT II show amplitudes that are too high, in particular with increasing frequencies. In some cases one can also observe shifts of the resonance positions from their correct positions. Of course, in the presented spectra one also can identify the eigenresonances of the conductor itself. In Fig. 3 below they appear at 167 and 335 MHz.

The positions of the resonance maxima/minima depend on the value  $Z_2$  of the impedance at the end of the conductor. Changing  $Z_2$  from very low (short – circuited) to very high (open circuit) values causes a shift of the resonance positions of  $\lambda/4$ . Furthermore, a reduction of



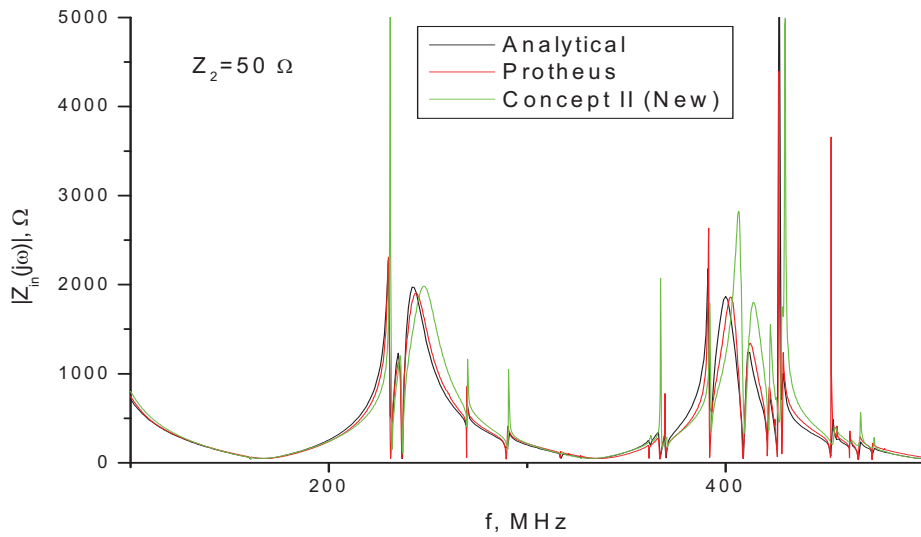


**Fig. 4** Exact calculation of  $Z_{in}$

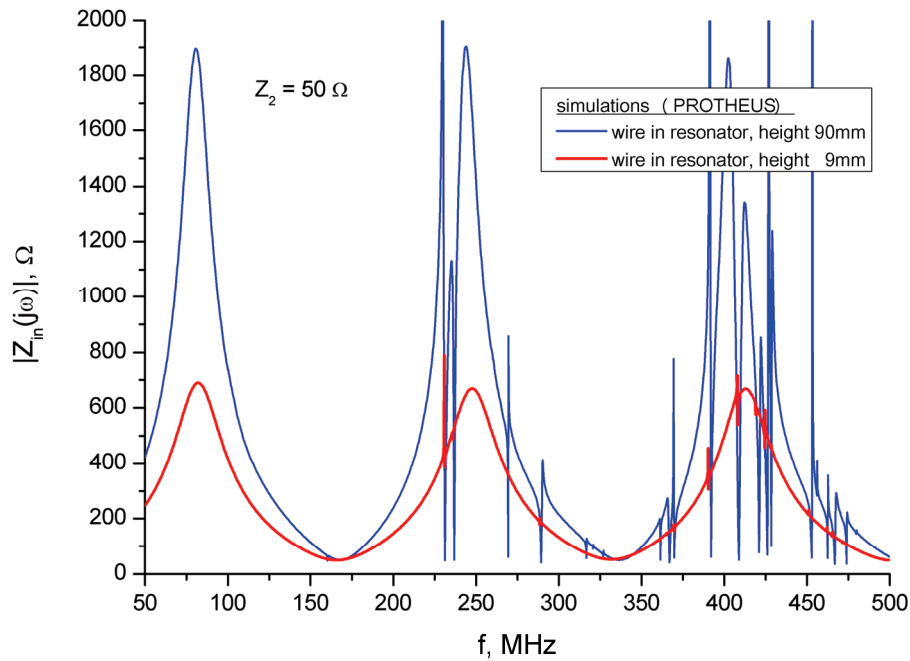


**Fig. 5** Frequency dependencies of impedance curves for different heights

the height of the line above ground (decrease of  $x_0$ ) changes the input – impedance curve in such a way that with decreasing  $x_0$  the amplitudes and the widths of the resonator peaks get smaller and, likewise, the impact (energy transfer) of the cavity on the conductor also decreases (see Fig. 5).

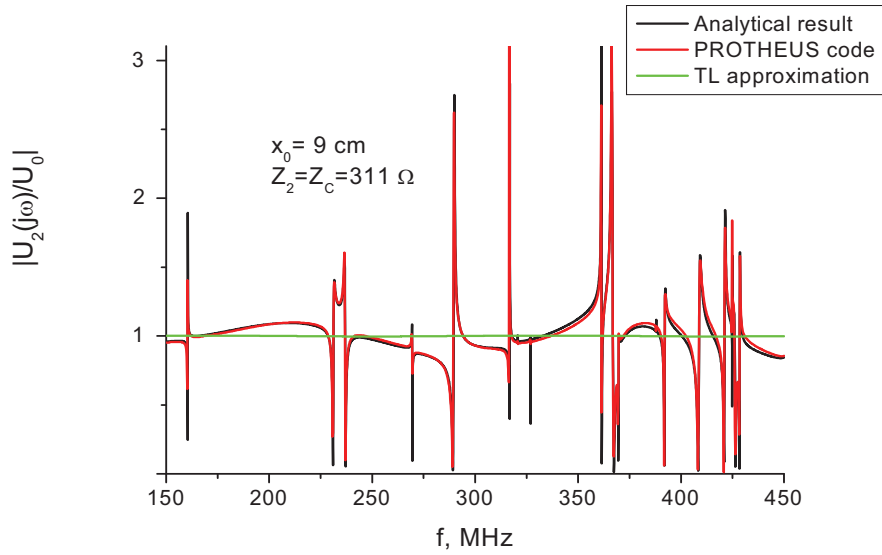


**Fig. 6** Frequency dependence of the transfer function

In addition to the input impedance also the voltage transfer function is of interest. It can be defined as a ratio of the voltage  $U_2$  across the load  $Z_2$  to the exciting voltage  $U_1$ . This function defines the transfer of a signal through the wire system. For the matched load  $Z_2=Z_C$  in the classical transmission line theory this transfer function just reduces to a phase shift, but for the line in the resonator the results can be quite different (see Fig. 6). In Fig.6 one can see again a good agreement between analytical theory and the result of PROTHEUS code). This result can be useful, for example, for the investigation of transmission lines inside cars and aircrafts.

Of course, a confirmation of the above calculations by an experiment would be desirable. First experiments have been conducted in which the input impedance ( $I(0)$ ) was measured.

A copper wire was soldered with both ends to the inner pin of male N connectors, and a network analyzer was used to measure the scattering parameters. To obtain the input impedance a one-port experiment was sufficient in which the scattering parameter  $S_{11}$  was measured. In a two-port measurement the current transfer ratio along the line was measured. Again a male N measurement cable was used for the connection of the network analyzer. For the connection of the end of the wire another cable had to be used. Both feedthroughs and the cables were calibrated before the experiment. The analysis of these experiments showed a good agreement with the analytical and numerical results. The measurement of the current along the line becomes more complicated since the connection to the current probe inside the resonator is complicated. The results of these experiments will be published in a separate paper (IN).

## 6. Conclusion.

The focus of the above consideration was placed on the interaction between a current carrying conductor inside a resonator (shielded room) and the resonator itself. In order to describe this interaction the Green's function of the resonator was used, which was derived by the mirror principle. The layout of the conductor was chosen such that it runs parallel to four of the

resonator walls and connects the other two. Therefore, the translation symmetry in one direction ( $z$  – direction) was retained. This fact simplified the representation of the electric field component that excited the conductor and the current distribution along the line. In both cases Fourier series for the spatial coordinate  $z$  were used. The unknown Fourier expansion coefficients ( $E_{z,n_3}^0, I_{n_3}$ ) were determined by the boundary condition for the total  $z$ -component of the electric field on the surface of the conductor. If the wire would not be conducted parallelly to four of the walls then the theory can be extended to that described in Refs. [23,24,28]. There, however, the Green's function of the cavity had to be used.

Both kinds of excitations of the conductor were permitted: with distributed sources (field – excitation) and/or with lumped sources. This is the usual case when devices in a shielded room are connected by cables. The obtained analytical and comparative numerical results demonstrate a very good agreement and a strong coupling between resonator and cable. In the calculated input impedance representations of the wire, typical resonance frequencies of the resonator show up. The energy absorption of the cable from the resonator field is particularly evident in the area of its natural frequencies. Cable conduction close to a wall will reduce this effect. Overall, it is clear that, as expected, the electromagnetic interactions strongly depend on the final operative environment of an electrical and/or electronic device.

As distributed sources that excite the cable inside the resonator one may imagine electromagnetic fields which penetrate from outside through apertures into the shielded room or those which are generated from the equipment inside the resonator, like, e.g., adjacent conductors.

Future research inside enclosures will include experiments and different geometries of shielded rooms. Of special interest is the cylindrical cavity which represents a basic model for a missile. Further filling of housing with equipment (like many cables and electronic components) will reduce its quality factor, and, therefore, part of the interior electromagnetic field energy is absorbed by the entire environment. As a consequence, the coupling of the exterior field to a chosen cable is also diminished.

## Acknowledgement

The authors would like to thank Dr. D. Giri for his carefully reading of the manuscript and his fruitful comments.

## References

- [1] F.M. Tesche, M. Ianoz and T. Karlsson, *EMC Analysis Method and Computational Models*, Wiley, 1997.
- [2] “Analysis and design of ultra wideband and high-power microwave pulse interactions with electronic circuits and systems”, *MURI AWARD F49620-01-1-0436*, CD and <http://www.ece.uic.edu/MURI-RF/>.
- [3] S.V.Tkatchenko, G.V.Vodopianov, L.M. Martynov, "Electromagnetic field coupling to an electrically small antenna in a rectangular cavity", *13<sup>th</sup> International Zurich Symposium and Technical Exhibition on Electromagnetic Compatibility*, February 16-18 1999, pp.379-384.
- [4] L.K. Warne, K.S.H. Lee, H.G. Hudson, W.A. Johnson, R.E. Jorgenson, and S.L. Stomach, “Statistical Properties of Linear Antenna Impedance in an Electrically Large Cavity”, *IEEE Trans. Ant. Prop.*, vol. 51, no 5, pp.978-991, May 2003.
- [5] S.Tkachenko, F.Gronwald, H.-G.Krauthäuser, J. Nitsch, “High Frequency Electromagnetic Field Coupling to Small Antennas in Rectangular Resonator”, *V International Congress on Electromagnetism in Advanced Applications (ICEAA)*, 15-19 September, 2009, pp. 74-78.

- [6] S. Tkachenko, J. Nitsch, M. Al-Hamid, „Hochfrequente Feldeinkopplung in kleine Streuer innerhalb eines rechtwinkligen Resonators“, „*Internationale Fachmesse and Kongress für Elektromagnetische Verträglichkeit*“, 09.-11. März 2010, Messe Düsseldorf“, ISBN 978-3-8007-3206-7, pp.121-128.
- [7] S. Tkachenko, J. Nitsch, R. Vick, “HF Coupling to a Transmission Line inside a Rectangular Cavity”, in Transactions of *URSI International Symposium on Electromagnetic Theory*, Berlin, Germany, August 16-19, 2010.
- [8] N.I. Nosich, “The method of analytical regularization in wave scattering and eigenvalue problems: Foundations and review of solutions”, *IEEE AP Mag.* vol. 41, pp. 34–39, June 1999.
- [9] G. Spadacini, S. A. Pignari, and F. Marliani, “Closed-Form Transmission Line Model for Radiated Susceptibility in Metallic Enclosures”, *IEEE Trans. Electromag. Compat.*, vol. EMC - 47, no. 4, pp. 701-708, Nov. 2005.
- [10] T. Konefal, J. F. Dawson, A. C. Denton, T. M. Benson, C. Christopoulos, A. C. Marvin, S. J. Porter, and D. W. P. Thomas, “Electromagnetic coupling between wires inside a rectangular cavity using multiple-mode analogous - transmission-line circuit theory,” *IEEE Trans. Electromagn. Compat.*, vol. EMC-43, no. 3, pp. 273–281, Aug. 2001.
- [11] T. Konefal, J. F. Dawson, A. C. Marvin, M. P. Robinson, S.J. Porter, “A Fast Multiple Mode Intermediate Level Circuit Model for the Prediction of Shielding Effectiveness of a Rectangular Box Containing a Rectangular Aperture”, *IEEE Trans. Electromagnetic Compatibility*, Vol. 47, No. 4, Nov. 2005, pp. 678-691.
- [12] C.E. Baum, “Damping Electromagnetic Resonances in Equipment Cavities”, *Interaction Notes*, Note 613, 10 June 2010.
- [13] I. S. Shapiro, M.A. Olshanetzki, *Topological Lectures for Physicists*, Moscow, 1999 (in Russian)
- [14] D.I. Wu and D.C. Chang, “A hybrid representation of the Green’s function in an overmoded rectangular cavity,” *IEEE Trans. Microw. Theory Tech.*, vol. MTT-36, no. 9, pp. 1334–1442, Sep. 1988.
- [15] S.V.Tkatchenko, G.V.Vodopianov, L.M. Martynov, "On the theory of the short - rise pulse penetration into rectangular cavities," *11<sup>th</sup> International Zurich Symposium and Technical Exhibition on Electromagnetic Compatibility*, March 7 - 9, 1995, pp.513 - 518.
- [16] J. Nitsch, S. Tkachenko, and S. Potthast, „Pulsed Excitations of Resonators“, *Interaction Notes*, Note 619, 30 September 2010.
- [17] S.G.T. Markov, A.F. Chaplin, *Excitation of Electromagnetic Waves*, Moscow, “Radio I Svjaz’ ”, 1983 (Russian) (“Vozbujshdenie Elektromagnitnuh Voln”).
- [18] A.P. Prudnikov, Yu.A. Brychkov, O.I. Marichev, *Integrals and series. Vol.- 1: Elementary functions*, Gordon & Breach, 1986.
- [19] A.P. Prudnikov, Yu.A. Brychkov, O.I. Marichev, *Integrals and series. Vol.- 2: Special functions*, Gordon & Breach, 1986.
- [20] M.Leontovich, M. Levin, “The theory of the excitation of oscillations in dipole antennas”, *Journal Technical Physics*, vol. XIV, No 9, pp. 481-506, 1944 (in Russian).
- [21] H.-D. Brüns, A. Freiberg and H. Singer, *CONCEPT-II Manual of the Program System*, TU Hamburg-Harburg, Feb. 2011
- [22] D. Wulf, R. Bunger, J. Ritter and R. Beyer, *Accelerated simulation of low frequency applications using PROTHEUS/MLFMA*, 2<sup>nd</sup> International ITG Conference on Antennas, München, Mar. 2007, p. 240.
- [23] J. Nitsch, F. Gronwald, and W. Wollenberg, *Radiating Nonuniform Transmission-Line Systems and the Partial Element Equivalent Circuit Method*, Wiley, 2009.
- [24] J. Nitsch, S. Tkachenko, *High-Frequency Multiconductor Transmission-Line Theory*, *Found. Phys.* (2010) 40, 1231-1252.
- [25] M. Abramowitz, I.A. Stegun, *Handbook of mathematical functions*, Dover, 1974.

- [26] R. Courant, D. Hilbert, *Methoden der Mathematischen Physik*, Springer, 1993.
- [27] V. Katrich, F. Novokhatskiy, “Integral Representations of the Green’s Function for the Helmholtz Equation in Parallel Plate, Rectangular Waveguide and Resonator”, Proceedings of the 11<sup>th</sup> International Conference on Mathematical Methods in Electromagnetic Theory, 11 September 2006, Kharkov, Ukraine.
- [28] J.B.Nitsch, S.V.Tkachenko, “Global and Modal Parameters in the Generalized Transmission Line Theory and Their Physical Meaning”, *Radio Science Bulletin*, **312**, March 2005, pp.21-31.
- [29] Y. Leviatan, A.T. Adams, “The response of two-wire transmission line to incident field and voltage excitation including the effects of higher order modes”, *IEEE Trans. Ant. Prop.*, Vol. Ap- 30, No. 5, Sept. 1982, pp.998-1003.

## Appendix I

### Representation of the function S through the Jacobi Theta – Function

In this Appendix a different representation for the function  $S$  is derived demonstrating the near resonance frequency dependence in explicit form. This helps to analyze frequency shifts of the resonances caused by interaction with a transmission line. Using a simple identity for the denominator of (14)

$$\frac{1}{k_v^2 - k^2 + j\delta} = \frac{1}{k_v^2 + j\delta} + \frac{1}{k_v^2 + j\delta} \cdot \frac{k^2}{k_v^2 - k^2 + j\delta} \approx \frac{1}{k_v^2} + \frac{1}{k_v^2} \cdot \frac{k^2}{k_v^2 - k^2 + j\delta} \quad (\text{AI.1})$$

one can re-write equation (14) for  $S(k, \vec{\rho}, \vec{\rho}')$  as<sup>5</sup>

$$S(k, \vec{\rho}, \vec{\rho}') = S_1(\vec{\rho}, \vec{\rho}') + S_2(k, \vec{\rho}, \vec{\rho}') \quad (\text{AI.2})$$

$$\text{where } S_1(\vec{\rho}, \vec{\rho}') := \frac{4}{ab} \sum_{n_1, n_2=1}^{\infty} \frac{\sin(k_{vx}x) \sin(k_{vx}x') \sin(k_{vy}y) \sin(k_{vy}y')}{k_v^2} \quad (\text{AI.3a})$$

and

$$S_2(k, \vec{\rho}, \vec{\rho}') := \frac{4k^2}{ab} \sum_{n_1, n_2=1}^{\infty} \frac{\sin(k_{vx}x) \sin(k_{vx}x') \sin(k_{vy}y) \sin(k_{vy}y')}{k_v^2 (k_v^2 - k^2 + j\delta)} \quad (\text{AI.3b})$$

The spatial dependence of the sum  $S_2$  is smooth for near coordinate values of the source point and the observation point; however, it contains all singularities in the frequency domain in explicit form. Instead of that, the sum  $S_1$  is frequency – independent, but it is singular in the space domain. Below it is demonstrated how one can extract the singularity. To do that the

---

<sup>5</sup> Note that such splitting procedure is equivalent (if one multiplies the summands by the trigonometric functions  $\cos(k_z^v z) \cos(k_z^v z')$  and carries out the summation over the index  $n_3$ ) to a splitting of the Green’s function for the vector potential in Lorenz gauge into the Green’s function in the Coulomb gauge and the difference between the two gauges (see, for example, [4]).

trigonometric functions in (AI.2) are presented as a sum of exponential functions, and an integral representation (AI.4) of the denominator in (AI.3a) is used.

$$\frac{1}{k_v^2} = \int_0^\infty \exp(-tk_v^2) dt = \int_0^\infty \exp\left[-t\left((\pi n_1/a)^2 + (\pi n_2/b)^2 + (\pi n_3/h)^2\right)\right] dt, \quad [t] = [L]^2 \quad (\text{AI.4})$$

Then the summation under the integration decouples, and after rearranging the sum one obtains for  $S_1$

$$S_1(\vec{\rho}, \vec{\rho}') = \frac{1}{4ab} \int_0^\infty e^{-t(\pi n_3/h)^2} \cdot \left[ \sum_{n_1=-\infty}^\infty e^{-t\left(\frac{\pi n_1}{a}\right)^2 + j\frac{\pi}{a}n_1(x'-x)} - \sum_{n_1=-\infty}^\infty e^{-t\left(\frac{\pi n_1}{a}\right)^2 + j\frac{\pi}{a}n_1(x'+x)} \right] \cdot \left[ \sum_{n_2=-\infty}^\infty e^{-t\left(\frac{\pi n_2}{b}\right)^2 + j\frac{\pi}{b}n_2(y'-y)} - \sum_{n_2=-\infty}^\infty e^{-t\left(\frac{\pi n_2}{b}\right)^2 + j\frac{\pi}{b}n_2(y'+y)} \right] \quad (\text{AI.5})$$

Note that the single sums in (AI.5) can be evaluated from the Jacobi theta-function of the third kind [25] (AI.6), and one can write for  $S_1$ <sup>6</sup>:

$$\theta_3(x, q) = \sum_{n=-\infty}^\infty q^{k^2} e^{2jkx} = 1 + 2 \sum_{n=-\infty}^\infty q^{k^2} \cos(2kx), \quad q < 1 \quad (\text{AI.6})$$

$$S_1(\vec{\rho}, \vec{\rho}') = \frac{1}{4ab} \int_0^\infty e^{-t(\pi n_3/h)^2} \cdot \left[ \theta_3\left(\pi(x'-x)/2a, e^{-t\pi/a^2}\right) - \theta_3\left(\pi(x'+x)/2a, e^{-t\pi/a^2}\right) \right] \cdot \left[ \theta_3\left(\pi(y'-y)/2b, e^{-t\pi/b^2}\right) - \theta_3\left(\pi(y'+y)/2b, e^{-t\pi/b^2}\right) \right] dt \quad (\text{AI.7})$$

As it was mentioned before, the sum  $S_1$  contains the spatial-divergent part. To extract this part, it is necessary to investigate the theta-functions in (AI.7) for small values  $|\vec{\rho}' - \vec{\rho}| \rightarrow 0$ . In this case one can show that the main contribution comes from small  $t$  values, and it is possible to change the summation by integration, for example, for the first term in the brackets (AI.7):

$$\sum_{n_1=-\infty}^\infty e^{-t\left(\frac{\pi n_1}{a}\right)^2 + j\frac{\pi}{a}n_1(x'-x)} \approx \int_{-\infty}^\infty dn_1 e^{-t\left(\frac{\pi n_1}{a}\right)^2 + j\frac{\pi}{a}n_1(x'-x)} = \frac{a}{\pi} \int_{-\infty}^\infty dk_x e^{-t(k_x^2) + jk_x(x'-x)} = \frac{a}{\pi} \sqrt{\frac{\pi}{t}} e^{-\frac{(x'-x)^2}{4t}} \quad (\text{AI.8})$$

After that one writes for eq. (AI.7)

---

<sup>6</sup> Here the Green's function of the two – dimensional Helmholtz equation with imaginary propagation constant (or Laplace equation for  $n_3=0$ ) was obtained with zero-boundary conditions for a rectangular region. For the three – dimensional Laplace equation for a rectangular region such consideration was carried out in the classical book [26]. For the three – dimensional Helmholtz equation (but with real propagation constant and without splitting (AI.2) in resonance and singular parts) for the rectangular region the Green's function was found in [27] as integral with the product of combined theta – functions  $\theta_3$ . The method in [27], however, requires a careful carrying out of the integration in the complex plane.

$$\begin{aligned}
S_1(\vec{\rho}, \vec{\rho}') &\underset{|\vec{\rho}' - \vec{\rho}| \rightarrow 0}{\approx} \tilde{S}_1(\vec{\rho}, \vec{\rho}') := \\
&\frac{1}{4ab} \int_0^\infty e^{-t\left(\frac{\pi n_3}{h}\right)^2} \frac{a}{\pi} \sqrt{\frac{\pi}{t}} \cdot \left[ e^{-\frac{(x'-x)^2}{4t}} - e^{-\frac{(x'+x)^2}{4t}} \right] \cdot \frac{b}{\pi} \sqrt{\frac{\pi}{t}} \cdot \left[ e^{-\frac{(y'-y)^2}{4t}} - e^{-\frac{(y'+y)^2}{4t}} \right] dt = \\
&= \frac{1}{4\pi} \int_0^\infty \frac{dt}{t} e^{-t(k_z^v)^2} \left[ e^{-\frac{(x'-x)^2+(y'-y)^2}{4t}} - e^{-\frac{(x'-x)^2+(y'+y)^2}{4t}} - e^{-\frac{(x'+x)^2+(y'-y)^2}{4t}} + e^{-\frac{(x'+x)^2+(y'+y)^2}{4t}} \right] = \\
&= \frac{1}{2\pi} \begin{cases} \left[ K_0\left(k_z^v \sqrt{(x'-x)^2+(y'-y)^2}\right) - K_0\left(k_z^v \sqrt{(x'-x)^2+(y'+y)^2}\right) - \right. \\ \left. - K_0\left(k_z^v \sqrt{(x'+x)^2+(y'-y)^2}\right) + K_0\left(k_z^v \sqrt{(x'+x)^2+(y'+y)^2}\right) \right], & k_z^v \neq 0 \quad (\text{AI.9}) \\ \ln \left[ \frac{\sqrt{(x'-x)^2+(y'+y)^2} \cdot \sqrt{(x'+x)^2+(y'-y)^2}}{\sqrt{(x'-x)^2+(y'-y)^2} \cdot \sqrt{(x'+x)^2+(y'+y)^2}} \right], & k_z^v = 0 \end{cases}
\end{aligned}$$

Here  $K_0(z)$  is a modified Bessel function of the second kind of zeroth order. To obtain the first part of eq. (AI.9), eq. (AI.10) was used (see [18]). To derive the second part of the formula it is necessary to take the limit  $k_z^v \rightarrow 0$  for the sum of Bessel functions.

$$\int_0^\infty \frac{dt}{t} e^{-a^2 t - \frac{r^2}{4t}} = 2K_0(ar), \quad (\text{AI.10})$$

From the integral form of eq. (AI.9) one can observe, that for coinciding values of  $x, x'$  and  $y, y'$  this integral has a logarithmical divergence for small  $t$  which is suppressed by exponent terms when  $x, x'$  and  $y, y'$  do not coincide. Now, to regularize the exact function  $S_1(\vec{\rho}, \vec{\rho}')$  in (AI.7) one can add and subtract  $\tilde{S}_1$  from eq. (AI.7) and gets:

$$\begin{aligned}
S_1(\vec{\rho}, \vec{\rho}') &= \frac{1}{4ab} \int_0^\infty e^{-t(\pi n_3/h)^2} dt \cdot \left\{ \left[ \theta_3\left(\pi(x'-x)/2a, e^{-t\pi/a^2}\right) - \theta_3\left(\pi(x'+x)/2a, e^{-t\pi/a^2}\right) \right] \cdot \right. \\
&\cdot \left[ \theta_3\left(\pi(y'-y)/2b, e^{-t\pi/b^2}\right) - \theta_3\left(\pi(y'+y)/2b, e^{-t\pi/b^2}\right) \right] - \frac{ab}{\pi t} \cdot \left[ e^{-\frac{(x'-x)^2+(y'-y)^2}{4t}} - \right. \\
&\left. - e^{-\frac{(x'-x)^2+(y'+y)^2}{4t}} - e^{-\frac{(x'+x)^2+(y'-y)^2}{4t}} + e^{-\frac{(x'+x)^2+(y'+y)^2}{4t}} \right] \left. \right\} + \tilde{S}_1(\vec{\rho}, \vec{\rho}') \quad (\text{AI.11})
\end{aligned}$$

Note that function  $\tilde{S}_1$  of the right side in eq. (AI.11) contains a spatial logarithmical singularity (compare with eq. (22)), however, the integral part of  $S_1$  in (AI.11) is a regular function for  $|\vec{\rho}' - \vec{\rho}| \rightarrow 0$ . Now one can calculate the function  $S(x = x_0 + r_0, y = y_0, x' = x_0, y' = y_0)$  which defines the current in eq. (15). Choosing values  $x \neq x_1$  only in singular term, one has:



$$S(x = x_0 + r_0, y = y_0, x' = x_0, y' = y_0) = S_1(x_0, y_0, r_0) + S_2(k, x_0, y_0) \quad (\text{AI.12})$$

$$S_2(k, x_0, y_0) = \frac{4k^2}{ab} \sum_{n_1, n_2=1}^{\infty} \frac{\sin^2(k_{vx} x_0) \sin^2(k_{vy} y_0)}{k_v^2 (k_v^2 - k^2 + j\delta)} \quad (\text{AI.13})$$

$$S_1(x_0, y_0, r_0) = \frac{1}{4ab} \int_0^{\infty} e^{-t(\pi n_3/h)^2} dt \cdot \left\{ \left[ \theta_3(0, e^{-t\pi/a^2}) - \theta_3(\pi x_0, e^{-t\pi/a^2}) \right] \cdot \left[ \theta_3(0, e^{-t\pi/b^2}) - \theta_3(\pi y_0, e^{-t\pi/b^2}) \right] - \frac{ab}{\pi t} \cdot \left[ 1 - e^{-\frac{y_0^2}{t}} - e^{-\frac{x_0^2}{4t}} + e^{-\frac{x_0^2 + y_0^2}{t}} \right] \right\} + \tilde{S}_1(x_0, y_0, r_0) \quad (\text{AI.14})$$

$$\tilde{S}_1(x_0, y_0, r_0) = \frac{1}{2\pi} \begin{cases} K_0(k_z^v r_0) - K_0(2k_z^v x_0) - K_0(2k_z^v y_0) + K_0(2k_z^v \sqrt{x_0^2 + y_0^2}), & k_z^v \neq 0 \\ \ln \left[ \frac{2x_0 y_0}{r_0 \sqrt{x_0^2 + y_0^2}} \right], & k_z^v = 0 \end{cases} \quad (\text{AI.15})$$

Equations (AI.12) - (AI.15) give the desired representation of the function S, which demonstrates the explicit singularities in spatial and frequency domains. It can be used both for numerical summation by eq. (15) and for analytical estimations.

Using this representation one can evaluate the shift of resonances of the induced current in comparison to the corresponding resonances for an empty cavity (for the short-circuit line). The current resonances are given by the zeros of the denominator in eq. (15). They can be divided into two sets: the line resonances which are given by the zeros of the first factor in the denominator. They coincide with the line resonances without cavity. Further there are the shifted cavity resonances which are given by the zeros of function S. To evaluate the latter resonances assume that  $r_0 \ll x_0 \ll y_0$ ,  $2\pi m_3 x_0 / h \ll 1$  and also that the frequency  $\omega$  is close enough to one of eigenfrequencies  $\omega_v$ . Keeping the leading terms in  $S_1$  and  $S_2$  one can write:

$$S \approx \frac{1}{2\pi} \ln(2x_0 / r_0) + \frac{4}{ab} \frac{\sin^2(k_x^v x_0) \sin^2(k_y^v y_0)}{k_v^2 - k^2} \quad (\text{AI.16})$$

The root of (AI.16) gives the shift of the resonance frequencies of the system “line in resonator” in comparison with the cavity eigenfrequencies.

$$\Delta\omega_v / \omega_v \sim \frac{4\pi \sin^2(k_x^v x_0) \sin^2(k_y^v y_0)}{abk_v^2 \ln(2x_0 / r_0)} \quad (\text{AI.17})$$



## Appendix II

### A one-dimensional sum representation of the function S

In this Appendix the function S is represented as a regularized one – dimensional sum with an extracted logarithmical singularity. This representation is convenient for the numerical calculations. To do that eq.(14) is re-written as

$$S(k, k_{vz}, \vec{\rho}, \vec{\rho}') = \sum_{n_2=1}^{\infty} \sin(k_{vy}y) \sin(k_{vy}y') \cdot S_{aux.}(k, k_{vz}, k_{vy}, x, x') \quad (\text{AII.1})$$

Where the auxiliary function  $S_{aux.}$  is defined by the sum

$$\begin{aligned} S_{aux.} &= S_{aux.}(k, k_{vz}, k_{vy}, x, x') := \frac{4}{ab} \sum_{n_1=1}^{\infty} \frac{\sin(k_{vx}x) \sin(k_{vx}x')}{k_{vx}^2 + \underbrace{k_{vy}^2 + k_{vz}^2 - k^2 + j\delta}_{:=\tilde{\gamma}_v^2}} = \\ &= \frac{2a}{b\pi^2} \sum_{n_1=1}^{\infty} \frac{\cos(n_1\pi/(x-x')/a) - \cos(n_1\pi(x+x')/a)}{n_1^2 + (a\tilde{\gamma}_v/\pi)^2} \end{aligned} \quad (\text{AII.2})$$

Using a formula for the cosine trigonometric sum (AII.3) [18]

$$\sum_{n=1}^{\infty} \frac{\cos(nx)}{n^2 \pm a^2} = \pm \frac{\pi}{2a} \left\{ \begin{array}{l} \cosh(a(\pi-x)) \cdot \text{csch}(\pi a) \\ \cos(a(\pi-x)) \cdot \text{csc}(\pi a) \end{array} \right\} \mp \frac{1}{2a^2} \quad (\text{AII.3})$$

one can write (keep in mind an imaginary value of  $\tilde{\gamma}_v$ )

$$S_{aux.} = \frac{2}{b} \frac{\sinh(\tilde{\gamma}_v(a-x_>)) \sinh(\tilde{\gamma}_v x_<)}{\tilde{\gamma}_v \sinh(\tilde{\gamma}_v a)} \quad (\text{AII.4})$$

where  $x_> = \max(x, x')$ ,  $x_< = \min(x, x')$ .

Then the equation (14) for function S becomes:

$$S(k, k_{vz}, \vec{\rho}, \vec{\rho}') = \frac{2}{b} \sum_{n_2=1}^{\infty} \sin(k_{vy}y) \cdot \sin(k_{vy}y') \cdot \frac{\sinh(\tilde{\gamma}_v(a-x_>)) \sinh(\tilde{\gamma}_v x_<)}{\tilde{\gamma}_v \sinh(\tilde{\gamma}_v a)} \quad (\text{AII.5})$$

The series (AII.5) converges for different values of arguments  $\vec{\rho}$  and  $\vec{\rho}'$ . It diverges when they coincide. The divergence appears during the summation for large  $n_2$ . To extract the divergent term in an explicit form the sum  $S_{aux.}$  for large  $n_2$  is considered:

$$S_{aux.}(k, k_{vz}, k_{vy}, x, x') : \underset{k_{vy}^2 \gg |k_{vz}^2 - k^2|}{\approx} \frac{1}{b} \frac{e^{-k_{vy}|x-x'|}}{k_{vy}} \quad (\text{AII.6})$$

This gives

$$\begin{aligned}
S(k, k_{yz}, \vec{\rho}, \vec{\rho}') &\sim \frac{1}{2\pi} \sum_{n_2=1}^{\infty} \frac{\cos(n_2\pi/(y-y')/b) - \cos(n_2\pi/(y+y')/b)}{n_y} e^{-n_y|x-x'|/b} = \\
&= \frac{1}{4\pi} \ln \left[ \frac{1 - 2e^{-\pi|x-x'|/b} \cos(\pi(y+y')) + e^{-2\pi|x-x'|/b}}{1 - 2e^{-\pi|x-x'|/b} \cos(\pi(y-y')) + e^{-2\pi|x-x'|/b}} \right] \quad (\text{AII.7})
\end{aligned}$$

During the calculation of (AII.7) a simple summation formula with complex  $\alpha$  ( $\text{Re } \alpha > 0$ ) is used which can be obtained by summation of geometric series and integration over parameter  $\alpha$ :

$$\sum_{n=1}^{\infty} \frac{\exp(-\alpha n)}{n} = \ln \left( \frac{1}{1 - \exp(-\alpha)} \right) \quad (\text{AII.8})$$

Adding and subtracting the infinite series (AII.7) to eq. (14) one gets

$$\begin{aligned}
S(k, k_{yz}, \vec{\rho}, \vec{\rho}') &= \frac{1}{b} \sum_{n_2=1}^{\infty} \sin(k_{yy}y) \cdot \sin(k_{yy}y') \cdot \left[ \frac{2 \sinh(\tilde{\gamma}_v(a-x_>)) \sinh(\tilde{\gamma}_v x_<)}{\tilde{\gamma}_v \sinh(\tilde{\gamma}_v a)} - \frac{1}{b} \frac{e^{-k_{yy}|x-x'|}}{k_{yy}} \right] + \\
&+ \frac{1}{4\pi} \ln \left[ \frac{1 - 2e^{-\pi|x-x'|/b} \cos(\pi(y+y')) + e^{-2\pi|x-x'|/b}}{1 - 2e^{-\pi|x-x'|/b} \cos(\pi(y-y')) + e^{-2\pi|x-x'|/b}} \right] \quad (\text{AII.9})
\end{aligned}$$

In this representation the logarithmic singularity is separated for closely adjacent values of the arguments. Then for the function S in the denominator of eq. (15) one can write:

$$\begin{aligned}
S(k, k_{yz}, x = x_0 + r_0, x' = x_0, y = y_0, y' = y_0) &= \\
\frac{1}{b} \sum_{n_2=1}^{\infty} \sin^2(k_{yy}y_0) \cdot \left[ \frac{2 \sinh(\tilde{\gamma}_v(a-x_0)) \sinh(\tilde{\gamma}_v x_0)}{\tilde{\gamma}_v \sinh(\tilde{\gamma}_v a)} - \frac{1}{k_{yy}} \right] &+ \frac{1}{2\pi} \ln \left[ \frac{b |\sin(\pi y_0)|}{\pi r_0} \right] \quad (\text{AII.10})
\end{aligned}$$

Equation (AII.10) gives the desired “one-dimensional sum” representation of the function S which explicitly shows the singularity in spatial coordinates. However, it contains singularities in frequency domain.

### Appendix III

#### Free space limit: $\mathbf{a, b, h} \rightarrow \infty$

It is of some interest to consider the limiting case  $\mathbf{a, b, h} \rightarrow \infty$  for the solution of the induced current (see eqs. (10),(15)). It is expected that the result is reduced to the well-known solution for the transmission line above perfectly conducting ground excited by an arbitrary (under some restriction) electrical field.

In order to approach this limit it is convenient to consider the two-dimensional filament representation of the function  $S$  (37) which - for the function in the denominator (15) - can be written as

$$\begin{aligned}
S(k, k_{vz}, x = x_0 + r_0, x' = x_0, y = y_0, y' = y_0) = \\
= \frac{1}{4\pi} G(k, k_{vz}) + \frac{1}{2\pi} \sum_{\substack{n_1, n_2 = -\infty \\ n_2 \neq 0, n_1 \neq 0, 1}}^{\infty} (-1)^{n_1 + n_2} \begin{cases} K_0(\gamma_{vz} | \bar{\rho} - \bar{\rho}(n_1, n_2) |), & k_{vz}^2 - k^2 > 0 \\ -\frac{j\pi}{2} H_0^{(2)}(\tilde{k}_{vz} | \bar{\rho} - \bar{\rho}(n_1, n_2) |), & k_{vz}^2 - k^2 < 0 \end{cases}
\end{aligned} \tag{AIII.1}$$

$$\text{with } G(k, k_{vz}) = \begin{cases} 2[K_0(\gamma_v r_0) - K_0(2\gamma_v x_0)], & k_{vz}^2 - k^2 > 0 \\ -j\pi[H_0^{(2)}(\tilde{k}_{vz} r_0) - H_0^{(2)}(2\tilde{k}_{vz} x_0)], & k_{vz}^2 - k^2 < 0 \end{cases} \tag{AIII.2}$$

It is assumed that the transversal dimensions of the resonator  $a$  and  $b$ , as well as the value  $y_0 \sim b$  tend to infinity, however, the height of the line above “ground”  $x_0$  remains finite. In the first step of calculations the length of the resonator  $h$  also remains finite. Then the term  $G(k, k_{vz})$ , which doesn't depend on  $a, b, y_0$  remains constant, but any term in the sum (AIII.1) containing  $a, b, y_0$  in its argument tends to zero according to the asymptotic properties of cylindrical functions [25]:

$$H_0^{(2)}(z) \underset{z \rightarrow \infty}{\approx} \sqrt{\frac{2}{\pi z}} e^{-j(z - \pi/4)}, \quad K_0(z) \underset{z \rightarrow \infty}{\approx} \sqrt{\frac{\pi}{2z}} e^{-z} \tag{AIII.3 a,b}$$

Then one obtains the following equation for the term (eq.(15)) and for current  $I(z)$  (eq.(10)):

$$I(z) = \sum_{n_3=0}^{\infty} I_{n_3} \cos(n_3 \pi z / h), \quad I_{n_3} = \frac{4\pi j k E_{zn_3}^0(x_0, y_0)}{\eta_0 (k_{vz}^2 - k^2) G(k, k_{vz})} \tag{AIII.4 a,b}$$

where the terms in the Fourier series for the electrical field are given by

$$E_{zn_3}^0(x_0, y_0) = \frac{\mathcal{E}_{n_3,0}}{h} \int_0^h E_z^0(x_0, y_0, z) \cos(n_3 \pi z / h) dz \tag{AIII.5}$$

If the function  $E_z^0(x_0, y_0, z)$  is continued for negative  $z$ , it becomes obvious that for the considered problem this function is even. As a consequence of this the summation over the index  $n_3$  of the Fourier terms  $E_{zn_3}^0(x_0, y_0)$  and  $I_{n_3}$  can also be extended to negative indices. Then it is possible to re-write the results for the cosine Fourier series as:

$$I(z) = \sum_{n_3=-\infty}^{\infty} \tilde{I}_{n_3} \exp(-jn_3 \pi z / h), \quad \tilde{I}_{n_3} = \frac{4\pi j k \tilde{E}_{zn_3}^0(x_0, y_0)}{\eta_0 (k_{vz}^2 - k^2) G(k, k_{vz})} \tag{AIII.4 a,b}$$

$$\tilde{E}_{zn_3}^0(x_0, y_0) = \frac{1}{2h} \int_{-h}^h E_z^0(x_0, y_0, z) \exp(jn_3 \pi z / h) dz \tag{AIII.5}$$

Now assume that the length of the system tends to infinity,  $h \rightarrow \infty$ . Then one can replace the summation by integration:

$$I(z) = \sum_{n_3=-\infty}^{\infty} \tilde{I}_{n_3} e^{-jn_3\pi z/h} = \frac{h}{\pi} \sum_{n_3=-\infty}^{\infty} \tilde{I}_{n_3} e^{-jn_3\pi z/h} \frac{\pi}{h} \underset{h \rightarrow \infty}{=} \frac{h}{\pi} \int_{k_z=-\infty}^{\infty} \tilde{I}_{n_3} e^{-jk_z z} dk_z \quad (\text{AIII.6})$$

$$k_z := n_3\pi z / h$$

Finally one gets:

$$I(z) = \int_{k_z=-\infty}^{\infty} \frac{2jkE_z^0(x_0, y_0, k_z)}{\eta_0(k_z^2 - k^2)G(k, k_z)} e^{-jk_z z} dk_z, \quad (\text{AIII.7})$$

with

$$E_z^0(x_0, y_0, k_z) = \int_{-\infty}^{\infty} E_z^0(x_0, y_0, z) e^{jk_z z} dz \quad (\text{AIII.8})$$

This equation formally coincides with the well known expression for the current induced by the arbitrary exciting (incident plus reflected) field  $E_z^0(x_0, y_0, z)$  (see, for example [29], eq. (10), differential mode) field in the horizontal wire above perfectly conducting ground ( $x_0$  is the height of the wire). The difference is that one obtains (AIII.8) for the even field  $E_z^0(x_0, y_0, -z) = E_z^0(x_0, y_0, z)$  which is connected with the symmetry of our initial system. As usual for practical calculations one has to assume small losses in the wire (a small complex part of  $k$ ) for the proper path-tracing of specific points of denominator.